Power performance optimization and loads alleviation with active flaps using individual flap control

Vasilis Pettas, Thanasis Barlas, Drew Gertz and Helge A Madsen

Technical University of Denmark Department of Wind Energy, Aerodynamic Design
Risø Campus, Frederiksborgvej 399, 4000 Roskilde Denmark

Corresponding author: vas.pettas@gmail.com

Abstract. The present article investigates the potential of Active Trailing Edge Flaps (ATEF) in terms of increase in annual energy production (AEP) as well as reduction of fatigue loads. The basis for this study is the DTU 10 MW Reference Wind Turbine (RWT) simulated using the aeroelastic code HAWC2. In an industrial-oriented manner the baseline rotor is upscaled by 5% and the ATEFs are implemented in the outer 30% of the blades. The flap system is kept simple and robust with a single flap section and control with wind speed, rotor azimuth, root bending moments and angle of attack in flap's mid-section being the sensor inputs. The AEP is increased due to the upscaling but also further due to the flap system while the fatigue loads in components of interest (blade, tower, nacelle and main bearing) are reduced close to the level of the original turbine. The aim of this study is to demonstrate a simple and applicable method that can be a technology enabler for rotor upscaling and lowering cost of energy.

1. Introduction

The design trend in the wind turbine industry leads towards larger multi MW rotors where the reduction of design loads and aerodynamic optimization becomes more significant. The application of ATEFs is an important part of these concepts as has been shown in previous works [**1, 2**]. In the present work all simulation activities are based on HAWC2 aeroelastic code [**3**] using the verified flap model implementation **[4]** with the unsteady aerodynamics using the ATEF dynamic stall model implementation **[5]**. In order to calculate the loads according to the industrial standard for load certification, the calculations are based on DLC 1.2 NTM (as stated on IEC standard 61400-1, third edition) an overview of which is presented in **[6]** along with the post processing tools in **[7].** The assumption that the total fatigue is derived from this DLC is valid, since in the channels of interest more than 98% of the fatigue is attributed to DLC 1.2 NTM. In the same manner the AEP calculations are performed with different turbulence intensity values without yaw misalignment for all speeds with six turbulence seeds for each calculation point, since there is not a standardized method for numerical derivation of power curves. The approach in this work focuses on increasing AEP and reducing design fatigue loads to the original baseline load envelope using the active flap system in order to enable efficient rotor upscaling. This approach, along with a robust and simplified control implementation, establishes a close connection to a possible industrial application of such a system.

2. Wind turbine upscaling

The DTU 10 MW RWT **[8]** is considered as the baseline turbine. There have been investigations on the topic of upscaling multi-MW turbines and its limitations, an overview of which can be found at **[9, 10]**. In the present case in order to formulate a business case and get a clear picture of the flap implementation potential, all the components except from the rotor are kept the same with the baseline. The already highly aerodynamically optimized rotor, has the same hub in the upscaled case while the blades are elongated to a 5% total increase. In order to keep the same characteristics the solidity was kept the same as well as the airfoil profiles at the same non-dimensional positions. Hence, chord and thickness are increased to the same level while the structural properties are kept exactly the same (same mass per length, cross sectional stiffness etc.) leading to a same (performance wise) but 'softer' blade. The maximum power is limited to 10MW in order to lower the loads and utilize the same generator/electronics setup. Moreover, in order to be consistent with the upscaling procedures **[10]** and have a 'fair' case for the flaps the maximum steady state thrust of the upscaled rotor was decreased to the same level as the baseline by introducing an earlier pitch scheduling which in turn decreased slightly the rated wind speed. Finally, the gains of the DTU WE controller were tuned using the DTU HwacStab2 tool **[11, 12]**. The resulting key operational characteristics and dimensions of both original and upscaled rotors are shown in **Table 1.**

Initially, the baseline turbines (original and 5% upscaled) were simulated according to IEC Design Load Basis (DLB). The results show an increase of 2-10% for the fatigue loads in the channels investigated with the highest identified at the blade root bending moment channels where torsional moment MzBR is increased the most by 18%. Previous results in load alleviation potential using ATEFs **[13, 14, 16]** agree that this reduction margin can be feasible. In terms of AEP the difference for the class IA wind climate ($V_{mean} = 10\ m/s$) and 10% turbulence for all speeds is 3.41% while for the other turbine classes this increase becomes higher.

3. Implementation and control of ATEF

The flap configuration applied to the upscaled rotor involves one flap section at the last 30% of the blade (29.7 m) close to the tip with individual actuators for each blade. At this section of the blade the airfoil used is the FFA-W3-241 and the flaps are occupying the 10% of the chord. The variation of aerodynamic characteristics by the flap deflection is based on 2D CFD results from the in-house code EllipSys 2D **[17]** for a Reynolds number between $6 \cdot 10^6 - 12 \cdot 10^6$, for free transition with turbulence intensity 0.1, 3D corrected using Bak's model **[18]**. The deflection limit of the flap is +/- 15 degrees and the one-per-blade actuator dynamics are taken into account using a linear servo model in Hawc2 with a first order system **[19]**, using a time constant whose value is an investigated parameter.

Table 1. Comparison of key parameters of the baseline and upscaled turbines.

Parameter	DTU 10 MW RWT	Upscaled turbine
Wind Regime	IEC Class IA	Same
Control	Variable Speed/ Collective Pitch	Same
Cut in speed [ms^{-1}]	4	Same
Cut out speed [ms^{-1}]	25	Same
Rated Wind Speed [ms^{-1}]	11.4	11
Rated Power [MW]	10	Same
Rotor Diameter [m]	178.3	187.2
Hub Diameter [m]	5.6	Same
Hub Height [m]	119.0	Same
Drivetrain	Medium Speed, Multiple stage Gearbox	Same
Minimum Rotor Speed [rpm]	6.0	5.0
Maximum Rotor Speed [rpm]	9.6	9.2
Maximum Generator Speed [rpm]	480.0	459.3
Gearbox Ratio	50	Same
Maximum Tip Speed [ms^{-1}]	90	Same
Shaft Tilt Angle [deg]	5.0	Same
Rotor Precone Angle [deg]	-2.5	Same
Blade Prebend [m]	3.33	3.50
Rotor Mass [kg]	227,962	239,360
Nacelle Mass [kg]	446,036	Same
Tower Mass [kg]	628,442	Same

The main controller of the turbine (pitch and torque regulation) is the same as the baseline **[12]** with retuned gains to fit the upscaled rotor and earlier pitching scheduling to limit maximum thrust to the baseline level. The controller features both partial and full load operation as well as switching mechanisms between modes of operation, utilizing measurements of rotor speed, tower accelerations and pitch angles as inputs and the generator torque and collective pitch angle as outputs. The proposed flap controller is completely decoupled from the main controller and is divided into two parts.

3.1 AEP increase objective

The first involves the partial load operation of the turbine. The flap angle command for each blade is based on measurement of the angle of attack in the mid-flap section. This requires the derivation of the local angle of attack from an inflow or pressure sensor. Alternatively, a model-based estimation of the angle of attack from load measurements could be utilized. The control algorithm uses predefined parameters which are based purely on the known $\mathbf{C_L}$-$\boldsymbol{\alpha}$ polar and a tunable flap angle offset parameter, as seen in **Equation 1**.

$$\boldsymbol{\beta} = \frac{\boldsymbol{C_{L\alpha}}\cdot(\boldsymbol{\alpha}-\boldsymbol{\alpha_{set}})}{\boldsymbol{C_{L\beta}}} - \boldsymbol{C_{L\alpha}}\cdot\boldsymbol{\alpha_0} + \boldsymbol{\beta_{offset}} \quad (1)$$

$\mathbf{C_{L\alpha}}$ and $\mathbf{C_{L\beta}}$ are the lift slopes for variations in angle of attack and flap angle respectively and α_0 is the angle of attack for zero lift. The $\boldsymbol{\alpha}_{\mathbf{set}}$ is chosen as the angle for optimal gliding ratio $\mathbf{C_L/C_D}$. Then $\boldsymbol{\alpha}$ is the measured (or estimated) angle of attack at the mid-flap section which is the only controller input. The

$\boldsymbol{\beta_{offset}}$ can be chosen based on prior calculations. The flap system dynamics time constant $\boldsymbol{\tau}$ is also chosen as a tunable parameter in this case in order to optimize the required (slow) response of the flap.

The choice of optimal parameters for the flap controller ($\boldsymbol{\beta_{offset}}$ and $\boldsymbol{\tau}$) is based on derivation of the optimal flap angle (beta) variation from simulations using HAWC2. A full sweep parametrical study is carried out for each wind speed and a range of the two basic flap parameters. The comparison of achieved average power gain for the parametric sweep is shown in **Figure 1**. Maximum power extraction is achieved with a flap angle offset of -7.5 degrees for all cases. Increasing the flap system time constant is shown to improve performance, as then the flap actuator compensates to the system's phase delay observed between flap actions and actual change in forces applied as well as the delay between measured angle of attack and control inputs. The sensitivity analysis on the chosen time constant indicates that there is a clear optimum setting for $\boldsymbol{\tau}$ =10s in the whole range of below rated operating points. Moreover, angle of attack input signal is low pass filtered so that the flap does not react to high frequency variations.

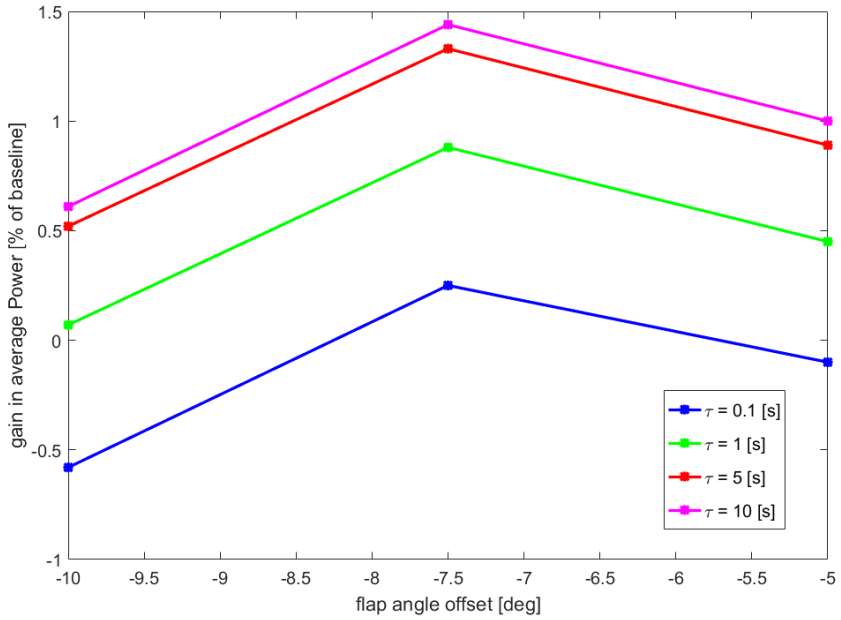

Figure 1. Average power gain for a range of flap offset angles and flap time constants.

3.2 Fatigue reduction objective

The second part of the controller is a classical Proportional Derivative (PD) individual flap controller. It is based on high-pass (HP) filtered flapwise blade root moment (MxBR) with a gain scheduling for proportional and derivative terms based on low-pass (LP) filtered wind speed, operating at the full load regime which was observed to contribute the most to the total fatigue damage equivalent load for the majority of the channels.

The MxBR signals pass through a HP filter in order to avoid flap reacting to steady and low frequency variations. Furthermore, a signal from main controller indicating full power is used in order to limit controller's actions to full load regime. This signal is a LP filtered indicator taking values between 0 and 1 (full load reached). Finally, the flap controller utilizes the main controller's grid status signal in order to assign a static angle when the turbine is not producing since it was decided not to operate the controller in parked cases.

The tuning method used in the present work consists of two parts. Firstly, a rough tuning is done using Ziegler-Nichols method **[20]** based on a high fidelity state space representation of the turbine (in open and closed loop) per speed obtained from HawcStab2. These gains along with their linear scheduling over wind speeds are shown in **Figure 2**. Subsequently, these values were manually tuned approximately for saturation limits based on a Matlab script including no-feedback and finally representative example cases were checked with results from applications of the controller in HAWC2 simulations. Finally, having the values from the previous step as a starting point parametrical studies were executed by running DLC 1.2 simulations in order to find the optimal gains for fatigue reduction. This control approach for load alleviation in full load regime has also been demonstrated and validated in previous works **[13, 14]**. Finally, the transition region is treated with a scaling factor added based on the full load indicator which makes sure that the flap controller is switching progressively from one region to another when operating close to rated speed.

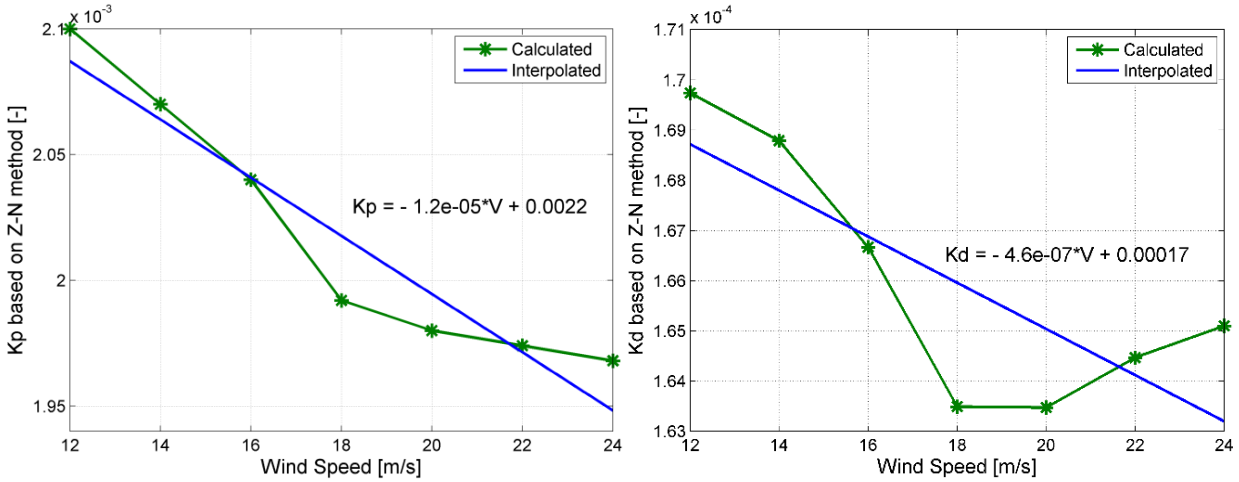

Figure 2. Proportional and Derivative term gains derived with Ziegler-Nichols method scheduled over wind speeds.

3.3 Integrated controller

The two parts of the controller are integrated in a holistic approach in order to realistically evaluate the load impact in the turbine lifetime, as well as, the influence in the individual effectiveness of each controller. The switching between the two controllers is based on wind speed and the rated power signal from the controller. When wind speed and rated indicator are below defined thresholds the AEP part is activated, while in all other cases (turbine producing power) the PD controller is active. These values were found with parametrical sweeps based on DLC 1.2 HAWC2 simulations in order to fulfill the objectives of smooth activity of the controller around rated speed and decoupling the control objectives so that the AEP increase and fatigue reduction is same as the individual applications. The block diagram of the integrated controller is shown in **Figure 3**.

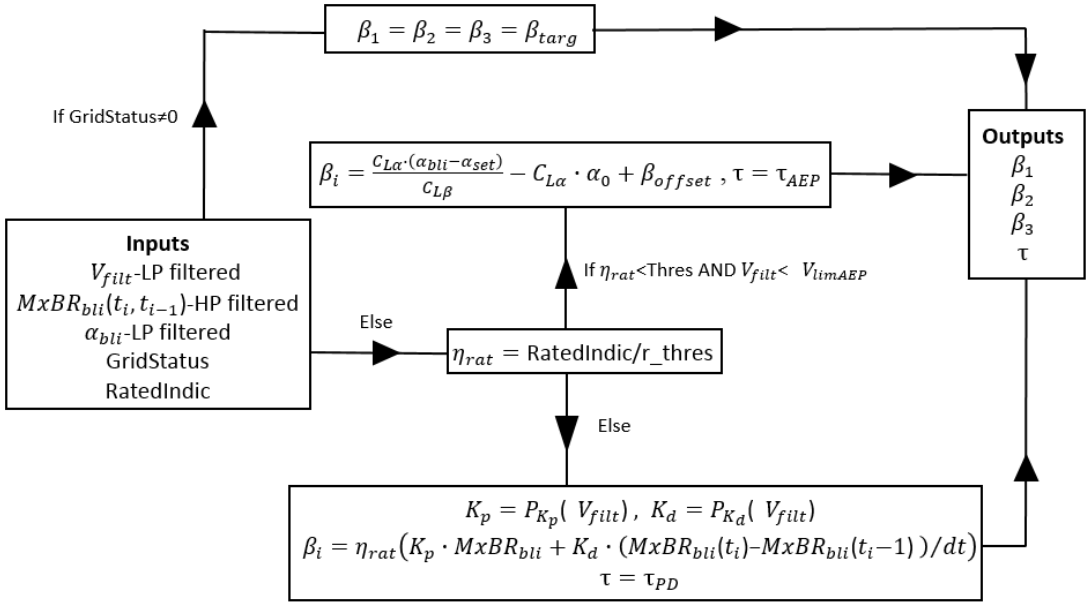

Figure 3. Flap controller's block diagram.

4. Results

The simulations were carried out at the baseline turbine as well as the upscaled with and without flaps while the controllers where applied both individually and integrated. The results indicate that the flap implementation can improve AEP up to 0.41% compared to the upscaled rotor. The AEP potential increase is evaluated with 10% turbulence intensity, as it is commonly performed in industry, where the flap contribution is found to be 0.19% while the total increase is 3.62%. All simulations were carried out with a wind shear exponent of 0.2, as stated in IEC standard, and tower shadowing effect included.

The comparison of power performance for every wind speed between all cases is shown in **Figure 4**. The variation of the achieved AEP for different turbulence intensity values is shown in **Table 2.** It is observed that the maximum AEP gain of 0.41% is achieved at the most ideal no turbulence conditions and decreases down to 0.11% when full IEC turbulence occurs. This is expected since the controller parameters are derived based on steady state simulations and as turbulence increases the non-linear effects become more dominant resulting to assignment of suboptimal flap angle values. The power increase trend is evident over the whole range of partial load region except for the transition regions at cut-in (where the turbine operates in an off-design point due to the constraints imposed by main controller for the rotational speed) and switching to full power.

Table 2. AEP results for compared cases.

case	flap angle offset [deg]	flap time constant [s]	turbulence intensity [%]	AEP gain [% 5% up baseline]	AEP gain [% original baseline]
1	-7.5	10	0	0.41	-
2	-7.5	10	5	0.25	-
3	-7.5	10	10	0.19	3.62
4	-7.5	10	IEC	0.11	3.51

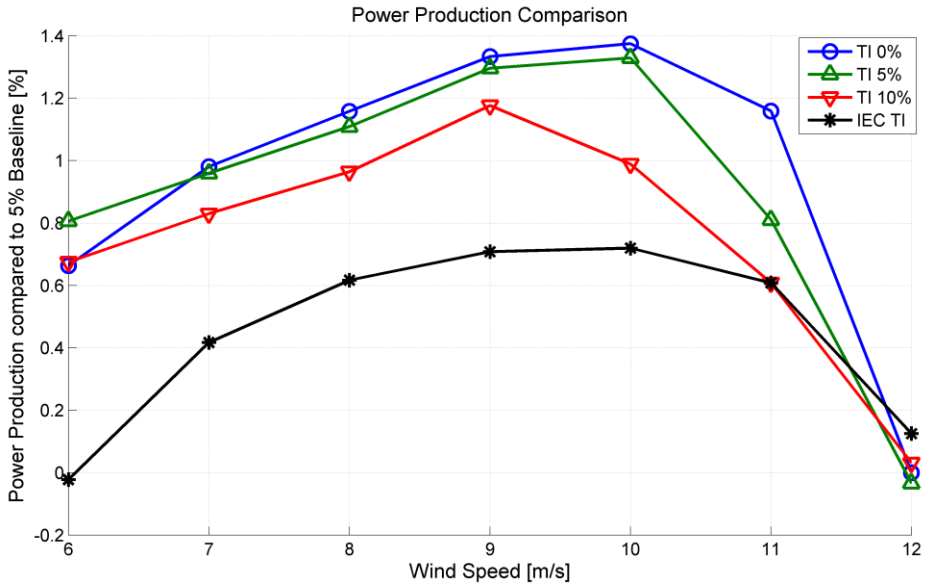

Figure 4. Power production per wind speed compared to 5% baseline with no flaps.

The previous results showed that the integrated controller reaches the same increase in AEP as the individual controller. Regarding the fatigue load reduction objective, results show that the trade-offs of this approach is mainly the small increase in the Damage Equivalent Loads (DEL) contributed from speeds below rated which is not possible to be compensated for by the PD part. This is in the level of 1-2% for most channels and only tower bottom channels are affected more in the level of 5-6%. The short term equivalent fatigue loads per wind speed shown in **Figure 5** for the main load channels can verify this observation where the fatigue loads over rated are decreased and below are increased due to the AEP part.

The PD controller alone (not shown), presents a decrease of 2%-15% to the lifetime fatigue loads (except for tower fore-aft, blade root edgewise and blade root torsion channels) close to the level of the baseline turbine and no influence to power generation. With the integrated controller applied, blade root bending moment and main bearing channels reach the baseline level while the tower loads are increased in the order of 2% to 4% due to the controller's AEP targeting operation. In above rated operation the reduction of the target blade root fatigue load is in the order of 10%, which brings the load level down to the baseline without upscaling. The blade root torsion is considerably increased, as expected, as a result of the increased aerodynamic pitching moment due to the flap operation. In general, the fatigue load targeting implementation suggested is found to be able to influence significantly MxBR and main bearing while the nacelle (tower-top) channels are less reduced when control is applied integrating both fatigue and AEP targeting modules. Tower bottom related channels are marginally decreased while blade and main bearing torsion channels seem to be only negatively affected by the flap implementation.

The lifetime fatigue equivalent loads comparison is shown in **Figure 6**. An overview of the abbreviations used in this figure and the corresponding load channels can be seen in **Table A1**. In general the integrated controller is a trade-off between power increase and load alleviation resulting in a 3.7% total increase in AEP while the fatigue loads in most channels are on the level of the baseline.

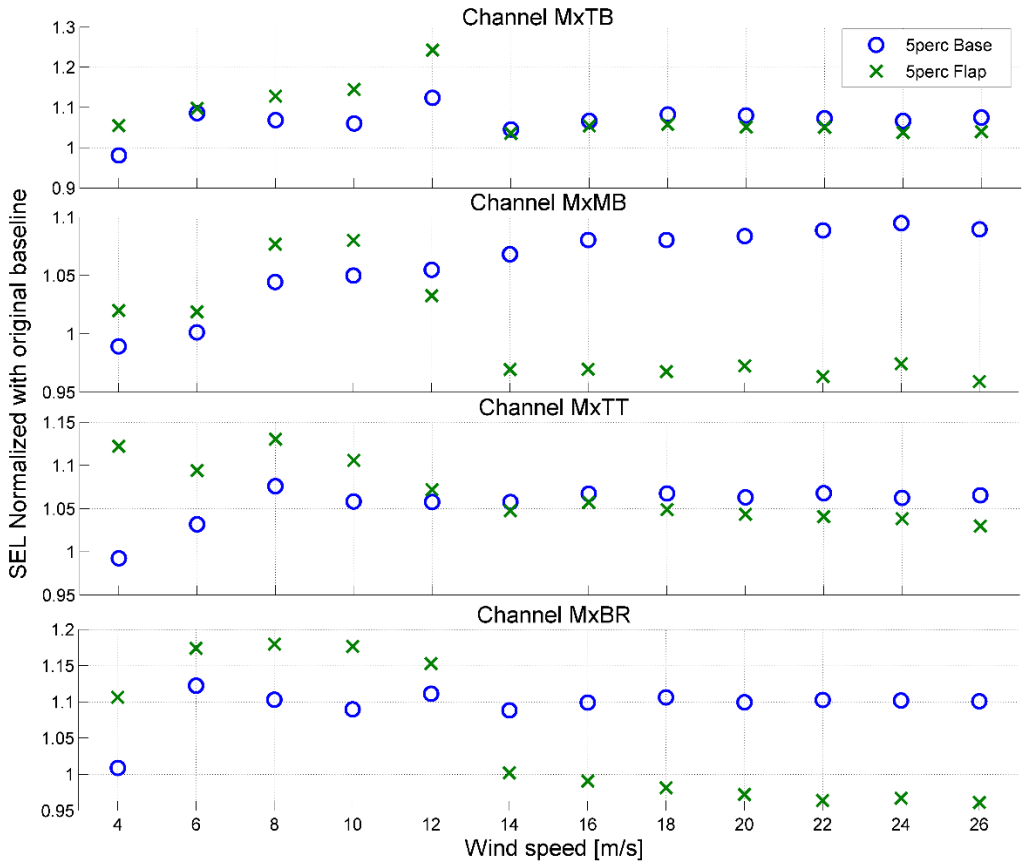

Figure 5. Short-term Equivalent Load (SEL) comparison to original baseline.

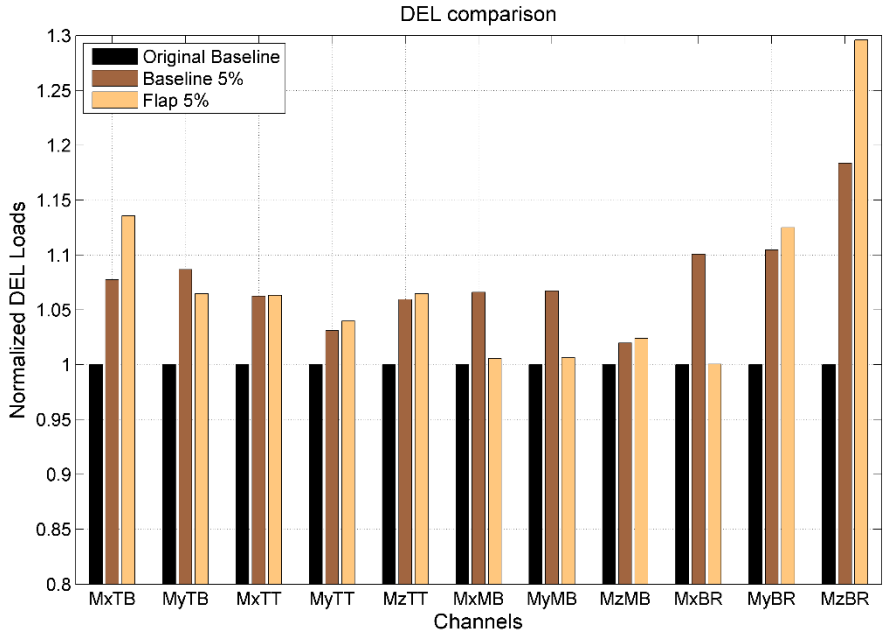

Figure 6. Comparison of lifetime equivalent fatigue loads on main channels for all cases.

5. Conclusions

The main conclusions are summarized below:

- In terms of AEP the individual flap control can increase AEP depending on the level of aerodynamic optimization of the rotor and the site-specific wind shear and turbulence intensity.
- The controller delivers significant fatigue load reduction in load channels of interest. The fatigue margin of the baseline components' design should be taken into account in order to evaluate whether the achieved reduction is sufficient to keep the same turbine platform.
- This control method is considered more robust and easy to apply than previous approaches since no significant increase to pitch activity is observed and the turbine–specific prescribed values are less prone to errors than other methods like model-based control algorithms.
- The presented flap controller approach establishes AEP increase and load reduction integration capability of the system in enabling further rotor upscaling.

Suggested future work should also consider the extreme load alleviation. A controller approach like a threshold cut-off could also be integrated in order to alleviate extreme loads which are another significant design driver. This fully integrated controller could reveal the full potential of a practical flap implementation in large rotor wind turbines.

Appendix

Table A1. Abbreviations of the load channels considered

Abbreviation	Load Channel
MxTB	Tower bottom fore-aft moment
MyTB	Tower bottom side-side moment
MxTT	Tower top tilt moment
MyTT	Tower top roll moment
MzTT	Tower top yaw moment
MxMB	Main bearing tilt moment
MyMB	Main bearing yaw moment
MzMB	Main bearing torsion
MxBR	Blade root flapwise moment
MyBR	Blade root edgewise moment
MzBR	Blade root torsion

Acknowledgments

The presented work is partly based on activities within the INDUFLAP2 project, funded by The Danish Ministry of Climate, Energy and Building, EUDP-2015-I, J.nr. 64015-0069 and with participation by Rehau, Siemens Wind Power and DTU.

References

[1] Barlas T K and van Kuik G A M Review of state of the art in smart rotor control research for wind turbines *Progress in Aerospace Sciences - 2010* **46** 1 pp 1-27 2010
[2] Madsen H A. et al. Towards an industrial manufactured morphing trailing edge flap system for wind turbines *Proceedings of EWEC 2014*, Barcelona, Spain 2014
[3] Larsen T J et al. How 2 Hawc2, the user's manual *Technical report, Risø-R-1597(ver. 4-4)(EN)* 2013
[4] Bergami L. Adaptive Trailing Edge Flaps for Active Load Alleviation in a Smart Rotor Configuration *PhD thesis*, DTU Wind Energy 2013
[5] Bergami L and Gaunaa M ATEFlap Aerodynamic Model, a dynamic stall model including the effects of trailing edge flap deflection *Technical report, Risø-R-1792(EN)* 2012
[6] Hansen M H et al. Design Load Basis for onshore turbines *Technical report*, *DTU Vindenergi-E-0174(EN)* 2015
[7] Pedersen, M. M., Post processing of Design Load Cases using Pdap *Technical report„ DTU Vindenergi-I-0371(EN)*, 2014.
[8] Christian Bak H et al. Description of the DTU 10 MW Reference Wind Turbine, *DTU Wind Energy Report-I-0092* 2013
[9] Sieros G et al. Upscaling wind turbines: theoretical and practical aspects and their impact on the cost of energy *Wind Energy, **15*** pp 3–17 2012
[10] UpWind Design limits and solutions for very large wind turbines, *UpWind EU project report* 2012
[11] Henricsen L C et al. HAWCStab2 User Manual *Technical report„ DTU Vindenergi (EN)*, 2015.
[12] Hansen M H et al. Basic DTU Wind Energy Controller, *DTU Wind Energy Report-E-0018* 2013
[13] Barlas et al. Load alleviation potential of active flaps and individual pitch control in a full design load basis, *Proceedings of the EWEA Annual Event and Exhibition* 2015
[14] Validation of new control concepts by advanced fluid-structure interaction tools, *Innwwind EU Project Deliverable 2.3.2* 2015
[15] Smit et al. Sizing and control of trailing edge flaps on a smart rotor for maximum power generation in low fatigue wind regimes. *Wind Energy, 19: 607–624* 2015
[16] Chen, Z. J. et al. System identification and controller design for individual pitch and trailing edge flap control on upscaled wind turbines. *Wind Energy, doi: 10.1002/we.1885*1 2015
[17] Sørensen, N. N. (2008). The EllipSys2D/3D code and its application within wind turbine aerodynamics [Sound/Visual production (digital)]. *Workshop on future aero-elastic tools for wind turbines*, Risø (DK) 2008
[18] C. Bak, J. Johansen, and P. B. Andersen. Three-dimensional corrections of airfoil characteristics based on pressure distributions. *Proc. European Wind Energy Conference and Exhibition (EWEC), 27. Feb. - 2. Mar. 2006, Athens, Greece*, 2006.
[19] T. Barlas and H. A. Madsen, Influence of actuator dynamics on the load reduction potential of wind turbines with distributed controllable rubber trailing edge flaps (CRTEF) *Proceedings of ICAST2011, pp. 1–12, 2011.*
[20] Z. JG and N. Nichols, Optimum settings for automatic controllers *Trans. ASME, no. **64**, pp. 759–768, 1942*.